

The stellar β -decay rate of ^{134}Cs and its impact on the Barium nucleosynthesis in the s process

KUO-ANG LI,^{1,2} CHONG QI,³ MARIA LUGARO,^{4,5,6} ANDRÉS YAGÜE LÓPEZ,⁴ AMANDA I. KARAKAS,^{6,7}
JACQUELINE DEN HARTOGH,⁴ BING-SHUI GAO,^{1,2} AND XIAO-DONG TANG^{1,2,8}

¹CAS Key Laboratory of High Precision Nuclear Spectroscopy, Institute of Modern Physics, Chinese Academy of Sciences, Lanzhou 73000, People's Republic of China

²School of Nuclear Science and Technology, University of Chinese Academy of Sciences, Beijing 100049, People's Republic of China

³Department of Physics, Royal Institute of Technology, Stockholm, Sweden

⁴Konkoly Observatory, Research Centre for Astronomy and Earth Sciences, Eötvös Loránd Research Network (ELKH), Konkoly Thege Miklós út 15-17, H-1121 Budapest, Hungary

⁵ELTE Eötvös Loránd University, Institute of Physics, Budapest 1117, Pázmány Péter sétány 1/A, Hungary

⁶School of Physics and Astronomy, Monash University, VIC 3800, Australia

⁷ARC Centre of Excellence for All Sky Astrophysics in 3 Dimensions (ASTRO 3D), Canberra, ACT 2611, Australia

⁸Joint department for nuclear physics, Institute of Modern Physics and Lanzhou University, Lanzhou, China, 730000

Submitted to ApJL

ABSTRACT

We have calculated the stellar β -decay rate of the important s -process branching point ^{134}Cs based on the state of the art shell model calculations. At typical s -process temperatures ($T \sim 0.2\text{-}0.3$ GK), our new rate is one order of magnitude lower than the widely-used rate from Takahashi and Yokoi (hereafter TY87). The impact on the nucleosynthesis in AGB stars is investigated with various masses and metallicities. Our new decay rate leads to an overall decrease in the $^{134}\text{Ba}/^{136}\text{Ba}$ ratio, and well explains the measured ratio in meteorities without introducing the i process. We also derive the elapsed time from the last AGB nucleosynthetic event that polluted the early Solar System to be >28 Myr based on the $^{135}\text{Cs}/^{133}\text{Cs}$ ratio, which is consistent with the elapsed times derived from ^{107}Pd and ^{182}Hf . The s -process abundance sum of ^{135}Ba and ^{135}Cs is found to increase, resulting in a smaller r -process contribution of ^{135}Ba in the Solar System.

Keywords: Nuclear Reactions, Nucleosynthesis, Abundances, Stars: AGB and Post-AGB

1. INTRODUCTION

The ^{134}Cs stellar β -decay rate is crucial to understand the origin of the Ba isotopes. The competition between the neutron capture and the β -decay of ^{134}Cs determines the relative abundances of ^{134}Ba and ^{136}Ba , two pure s -process isotopes shielded by their stable xenon isobars, and influences the s -process nucleosynthesis of ^{135}Ba and ^{135}Cs . The astrophysical sites for the production of these two Ba isotopes in the Galaxy are asymptotic giant branch (AGB) stars with initial masses predominantly in the range $2\text{-}4 M_{\odot}$. The main neutron source is the $^{13}\text{C}(\alpha, n)^{16}\text{O}$ reaction activated in a thin region of the He-rich shell at $T \sim 0.1\text{GK}$ (Gallino et al. 1998; Travaglio et al. 1999; Karakas & Lattanzio 2014). The $^{22}\text{Ne}(\alpha, n)^{25}\text{Mg}$ reaction is also activated during the thermal instabilities associated with He burning in these stars at $T \sim 0.3\text{GK}$. It provides a peak neutron density orders of magnitude higher than that generated by the ^{13}C source: up to $10^{12\text{-}13} \text{ cm}^{-3}$ (^{22}Ne source) compared to $10^{7\text{-}8} \text{ cm}^{-3}$ (^{13}C source). As a result, the branching point ^{134}Cs is much more efficiently activated in the neutron flux provided by the ^{22}Ne than by the ^{13}C neutron source (Lugaro et al. 2003; Fishlock et al. 2014; Bisterzo et al. 2015). A typical s -process path is shown in Figure 1.

Corresponding author: Kuo-Ang Li
lika@impcas.ac.cn

Corresponding author: Chong Qi
chongq@kth.se

Corresponding author: Maria Lugaro
maria.lugaro@csfk.org

The rich variety of observations of the Ba and Cs isotopes in the Universe, which related to this branching, offers a number of opportunities to probe the nucleosynthesis at various sites: (i) It was found that two nominally mainstream SiC grains with strongly negative $\delta(^{134}\text{Ba}/^{136}\text{Ba})$ values could not be explained by any of the current AGB model calculations, suggesting that such negative values were consistent with the intermediate neutron capture process (*i*-process), whose neutron density is much higher than that of *s*-process, during the post-AGB stage (Liu et al. 2014). (ii) ^{135}Cs ($T_{1/2}=2.3$ Myr) is a long-lived isotope produced by AGB stars. It can be used to derive the elapsed time from the last AGB nucleosynthetic event that polluted the pre-solar system matter to the birth of the Sun (Brennecke & Kleine 2017). (iii) ^{135}Ba is produced in the *s*- and *r*-processes. A reliable prediction of the abundance sum of ^{135}Ba and its progenitor nucleus, ^{135}Cs , in AGB stars is important to determine the *r*-process contribution in the Solar System.

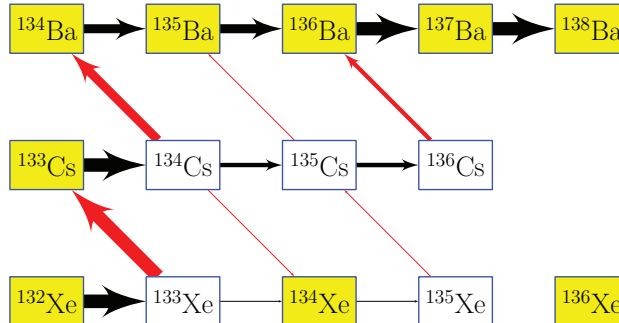


Figure 1. The *s*-process path at the vicinity of ^{134}Cs at $T = 0.35$ GK ($kT = 30$ keV) generated by the NUCNET code (Bojazi & Meyer 2014). The red lines present β -decay, while the black lines present the neutron capture. Line width indicates the flow current in linear scale. The stable nuclei are marked with yellow color.

A reliable β -decay rate of ^{134}Cs is essential for describing quantitatively the branching ratio and interpret correctly these nucleosynthetic outcomes. In stellar environments, the low-lying states of ^{134}Cs are thermally populated and contribute to the total β -decay rates. Takahashi and Yokoi calculated the beta decay rate of ^{134}Cs based on the empirical $\log ft$ values extracted from the outdated nuclear structure data in the 1980s (Takahashi & Yokoi 1987). By artificially varying the transition strengths, the uncertainty of the ^{134}Cs β -decay has been estimated to be of one order of magnitude (Goriely 1999). As the neutron capture cross sections on ^{134}Cs and $^{134,136}\text{Ba}$ are determined with errors better than 10% (Patronis et al. 2004; KADoNis v0.3), the uncertainty of the β -decay rate is the major limitation in the studies of the *s* process.

In this paper, we present a new stellar β -decay rate of ^{134}Cs deduced from the Gamow-Teller (GT) transition strength [$B(\text{GT})$] obtained from large-scale shell-model calculations. With the new β -decay rate, we investigate its impact on the nucleosynthesis using AGB stellar models covering various masses and metallicities.

2. CALCULATION OF THE β -DECAY RATE OF ^{134}CS IN THE STELLAR ENVIRONMENT

The terrestrial decay rate of ^{134}Cs has been well studied in the laboratory with a half-life of 2.0652(4) years. It is dominated by the β^- decay. Only a tiny fraction of the decay channels, 3×10^{-6} , is β^+ /electron-capture (EC) decay, which is negligible. In stellar environments, β -decays from thermally populated excited states could make a significant contribution to total decay rates. However, even at the *s* process temperatures, β^+ /EC decays contribute less than 1% of the total decay rate according to TY87. Due to its minor contribution, in the present work we focus on the β^- -decay channel and adopt TY87 rate for the β^+ -/EC channel.

Fig 2 shows the stellar β -decay scheme of ^{134}Cs . The terrestrial ^{134}Cs β -decay is dominated by transitions from the ^{134}Cs 4^+ ground state to the two 4^+ states of ^{134}Ba with excitation energies of 1401 and 1970 keV, respectively. Due to the small decay energies (658 and 89 keV), the terrestrial decay rate is relatively slow. However, with the thermal population of the excited states, the stellar β -decay rate could be significantly enhanced due to contributions from the two transitions, $(3^+, 60 \text{ keV}) \rightarrow (2^+, 605 \text{ keV})$ and $(1^+, 177 \text{ keV}) \rightarrow (0^+, \text{g.s.})$, in the *s*-process environment, due to the combination with high population possibility, high transition strength and the large decay phase space.

In the TY87 rate, the unknown transition strengths of the excited states were estimated from the analogous transitions in the existing experimental data, i.e., the transitions from the terrestrial β -decay of neighbouring nuclei.

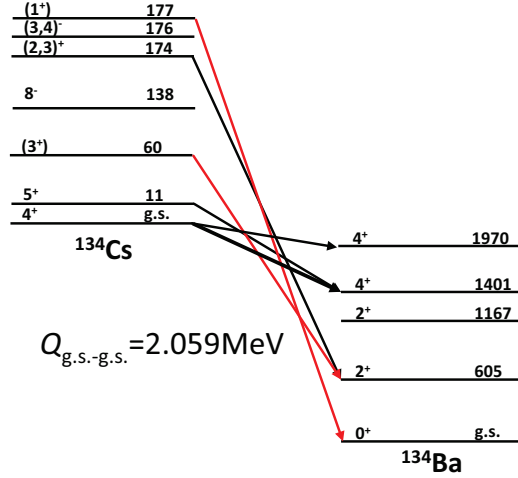


Figure 2. The stellar β -decay scheme of ^{134}Cs . The weak β^+ /EC channel is not shown. Only allowed transitions of excited states below 200keV are listed. The important transitions to low-lying states of ^{134}Ba are highlighted with red lines. The tentative J^π assignments are shown with parentheses.

Nowadays with the progress in computational nuclear physics, the transition strength can be calculated more precisely by using the large-scale nuclear shell model.

We have applied the large-scale shell model (hereafter SM) to calculate the transition strengths of the excited states and updated the stellar β -decay rate of ^{134}Cs . The large-scale shell model is a full configuration interaction approach that takes into account all possible couplings and correlations among valence nucleons within one or a few major shells. We assume ^{100}Sn as the inert core and consider the neutron and proton orbitals between the shell closures N (and Z) = 50 and 82, comprising $0g_{7/2}$, $1d_{5/2}$, $1d_{3/2}$, $2s_{1/2}$ and $0h_{11/2}$ orbitals. The starting point of our calculation is the realistic CD-Bonn nucleon-nucleon potential (Machleidt 2001). The interaction was renormalized using the perturbative G-matrix approach to take into account the core-polarization effects (Hjorth-Jensen et al. 1995). The $T = 1$ component of the monopole interaction was optimized by fitting the low-lying states of all Sn isotopes between ^{101}Sn and ^{132}Sn (see Ref. Qi & Xu (2012) for details). Our calculations in the present work reproduced the spectrum of ^{134}Ba and all the lying states of ^{134}Cs in Fig. 2 with recommended spin-parity assignments within ± 200 keV, though the orders can be slightly different. It is, however, not a major issue for the present work because the levels and their corresponding wave functions are identified based on their J^π values. The wave functions of ^{134}Cs and ^{134}Ba are calculated to be dominated by the coupling of protons in nearly degenerate $g_{7/2}d_{5/2}$ orbitals and neutrons in the $s_{1/2}d_{3/2}h_{11/2}$ orbitals. Those are consistent with the low-lying spectra of neighbouring odd-A $^{133,135}\text{Cs}$ and $^{133,135}\text{Ba}$. As a result, the GT strength mostly come from the transition $\pi d_{5/2}$ to $\nu d_{3/2}$.

With the updated $\log ft$ values calculated from the shell model, we obtained a new stellar β^- -decay rate of ^{134}Cs which is shown in Fig 3(a) along with TY87 rate. The new rate is about one order of magnitude slower than TY87 at the s -process temperatures.

The individual contributions of the major transitions in the total stellar β^- -decay rate of ^{134}Cs is presented in Fig 3(b). The $(3^+, 60 \text{ keV}) \rightarrow (2^+, 605 \text{ keV})$ transition ($\log ft = 7.8(\text{SM})$ vs. $6.5(\text{TY87})$) dominates, and the transition $(1^+, 177 \text{ keV}) \rightarrow (0^+, \text{g.s.})$ contributes only a minor fraction ($\log ft = 7.6(\text{SM})$ vs. $5.5(\text{TY87})$). To estimate the uncertainty of the transition strength calculated by the shell model calculation, we have done several calculations by slightly varying nucleon excitations from $g_{7/2}d_{5/2}$ to $s_{1/2}d_{3/2}h_{11/2}$ orbitals and the single-particle energies of the neutron $d_{3/2}$ orbital. In those calculations the calculated GT strength for the mostly relevant 3^+ to 2^+ decay vary mostly within a factor of two. As the most important transition $(3^+, 60 \text{ keV}) \rightarrow (2^+, 605 \text{ keV})$ is between two short lived excited states, our approach is the best way at present to obtain the strength.

One major source of the uncertainty of the ^{134}Cs decay rate comes from the spin-parity (J^π) assignments of the excited states. In our shell model calculations and TY87, the level scheme is taken from NNDC (2021). However, due to the limitations of experimental data, the J^π assignments of some states are still debated. $J^\pi = 3^+$ is suggested for the 60-keV state in which case the transition to the $(2^+, 605\text{keV})$ state in ^{134}Ba is allowed. However, other J^π values such as 4^+ could not be excluded (NNDC 2021; Bogdanović et al. 1987) resulting in a forbidden transition with

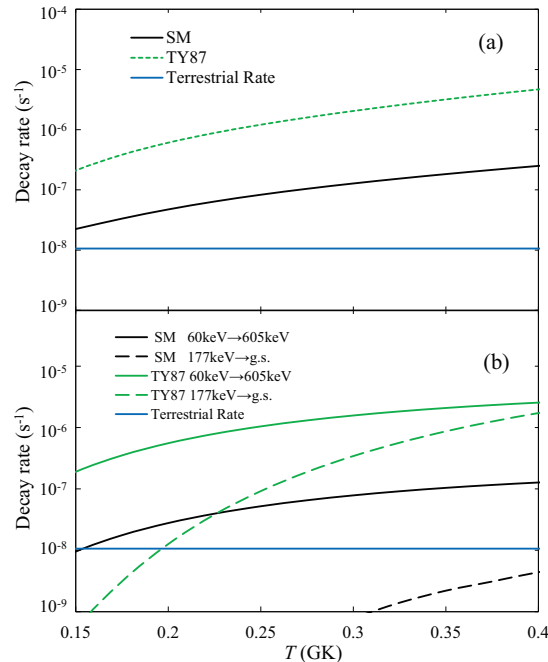


Figure 3. ^{134}Cs stellar β^- -decay rate of TY87 and the present work obtained with the shell model (SM)(a), and the decay rates of individual important transitions (b). The terrestrial rate is also presented.

a significant reduction in the total decay rate. A similar situation also exists for the 177-keV state. The transition from this state to the ^{134}Ba ground state will be of forbidden nature if its J^π is not 1^+ . Such ambiguity could be eliminated by further experiment such as the in-beam γ spectroscopy.

3. IMPACT OF NEW ^{134}CS β^- -DECAY RATE ON NUCLEOSYNTHESIS

To test the impact of the new decay rate presented here on the production of the Ba isotopes in the Galaxy, we have run several selected models of AGB nucleosynthesis for masses in the range 2 to $4.5 M_\odot$ and metallicities from 1/140 to twice solar metallicity (Lugaro et al. 2012; Karakas 2014; Karakas & Lugaro 2016; Karakas et al. 2018). A solar metallicity of 0.014 (Asplund et al. 2009) is adopted in the present work. As described in more detail in, e.g., Karakas & Lugaro (2016), our computational method is based on the post-processing nucleosynthesis code developed by Cannon (1993), where the changes in the abundances due to nucleosynthesis and mixing within convective regions are solved simultaneously. This means that we can treat the temperature dependence of the decay rate of ^{134}Cs together with mixing during the thermal instability where the ^{22}Ne neutron source is activated. In any case, our results appear generally robust considering that for our $^{134}\text{Ba}/^{136}\text{Ba}$ ratios are remarkably similar (within 10%) to those produced by the FRUITY models (Cristallo et al. 2009, 2011) for the same stellar masses and metallicities. The FRUITY models were calculated by interpolating the TY87 decay rates over the temperature of interest (i.e., not using an average value of the rate), but differently to our computations they solved separately the effects of nucleosynthesis and of the mixing.

The results of our models are presented in Table 1. Because the new decay rate is typically lower than the TY87 rate, e.g., roughly by a factor of ten at 270 MK (23 keV), the neutron capture of ^{134}Cs is more effectively activated in the models calculated with the new rate. As the ^{22}Ne reaction is dependent on the temperature in the He shell, which in turn increases with increasing stellar mass and decreasing metallicity, the significance of the impact of the new rate also increases with increasing stellar mass and decreasing metallicity. In summary, we obtained a significant decrease in the abundance of ^{134}Ba and ^{135}Ba by up to roughly 40%, a strong increase in ^{135}Cs (by roughly a factor 2 to 4), and no significant changes in the ^{136}Ba abundance, which indicates that the branching path rejoins the standard s-process path at this isotope, in other words, there is no further effect of the branching chain through the Cs isotopes on ^{136}Ba and ^{137}Ba . Interestingly, since ^{135}Cs eventually decays into ^{135}Ba , the final s-process ^{135}Ba abundance, i.e., the abundance sum of ^{135}Ba and ^{135}Cs , increases by up to 40%.

Table 1. Stellar surface abundances by number (in units of 10^{-11}) and isotopic ratios for selected Ba and Cs isotopes at the end of the evolution for our set of AGB models. Values in roman font are calculated using the ^{134}Cs decay rate by [Takahashi & Yokoi \(1987\)](#), while values given in italics are calculated using the decay rate from the present study, with the change indicated in brackets.

Mass (M_{\odot})	^{134}Ba	^{135}Ba	$^{135}\text{Ba}+^{135}\text{Cs}$	$(^{134}\text{Ba}/^{136}\text{Ba})/\odot$	^{135}Cs
Z = 0.03					
2.5	10.2, <i>9.53 (-7%)</i>	4.86, <i>4.67 (-4%)</i>	5.15, <i>6.00 (+16%)</i>	1.38, <i>1.25</i>	0.29, <i>1.33 ($\times 4.6$)</i>
2.75	10.6, <i>9.53 (-10%)</i>	5.06, <i>4.74 (-6%)</i>	5.55, <i>6.63 (+20%)</i>	1.33, <i>1.17</i>	0.49, <i>1.89 ($\times 3.8$)</i>
3	9.29, <i>7.93 (-15%)</i>	4.57, <i>4.13 (-10%)</i>	5.21, <i>6.46 (+24%)</i>	1.28, <i>1.08</i>	0.64, <i>2.33 ($\times 3.6$)</i>
3.5	4.67, <i>3.75 (-20%)</i>	2.87, <i>2.58 (-10%)</i>	3.47, <i>4.32 (+25%)</i>	1.22, <i>0.97</i>	0.60, <i>1.75 ($\times 2.9$)</i>
4	3.48, <i>2.46 (-29%)</i>	2.40, <i>2.00 (-17%)</i>	2.99, <i>3.73 (+25%)</i>	1.15, <i>0.82</i>	0.71, <i>1.79 ($\times 2.5$)</i>
4.5	1.07, <i>0.88 (-18%)</i>	1.59, <i>1.51 (-5%)</i>	1.73, <i>1.93 (+11%)</i>	1.12, <i>0.93</i>	0.17, <i>0.42 ($\times 2.4$)</i>
Z = 0.014					
2	10.5, <i>9.20 (-12%)</i>	4.43, <i>4.01 (-10%)</i>	4.97, <i>6.19 (+25%)</i>	1.28, <i>1.12</i>	0.54, <i>2.18 ($\times 4.0$)</i>
3	14.0, <i>10.6 (-24%)</i>	5.67, <i>4.65 (-18%)</i>	7.86, <i>10.7 (+37%)</i>	1.18, <i>0.90</i>	2.19, <i>6.10 ($\times 2.8$)</i>
3.5	7.84, <i>5.50 (-30%)</i>	3.34, <i>2.59 (-22%)</i>	5.52, <i>7.56 (+37%)</i>	1.16, <i>0.82</i>	2.18, <i>4.97 ($\times 2.3$)</i>
4	6.93, <i>4.18 (-40%)</i>	2.95, <i>1.83 (-38%)</i>	6.97, <i>9.37 (+34%)</i>	1.16, <i>0.71</i>	4.01, <i>7.54 ($\times 1.9$)</i>
4.5	2.32, <i>1.48 (-36%)</i>	1.40, <i>1.04 (-25%)</i>	2.72, <i>3.49 (+29%)</i>	1.11, <i>0.71</i>	1.32, <i>2.45 ($\times 1.8$)</i>
Z = 0.007					
2.5	14.8, <i>11.0 (-26%)</i>	5.77, <i>4.64 (-35%)</i>	8.50, <i>12.0 (+41%)</i>	1.08, <i>0.80</i>	2.72, <i>7.32 ($\times 2.7$)</i>
3	15.8, <i>10.3 (-20%)</i>	6.01, <i>4.48 (-25%)</i>	11.8, <i>16.6 (+41%)</i>	1.05, <i>0.69</i>	5.78, <i>12.1 ($\times 2.1$)</i>
Z = 0.0028					
3	4.92, <i>2.84 (-42%)</i>	1.93, <i>1.23 (-36%)</i>	5.67, <i>7.45 (+31%)</i>	1.04, <i>0.61</i>	3.74, <i>6.22 ($\times 1.7$)</i>
Z = 0.001					
2.5	1.90, <i>1.07 (-36%)</i>	0.75, <i>0.47 (-37%)</i>	2.01, <i>2.70 (+34%)</i>	1.06, <i>0.61</i>	1.26, <i>2.23 ($\times 1.8$)</i>
Z = 0.0001					
2.5	0.19, <i>0.11 (-42%)</i>	0.08, <i>0.05 (-37%)</i>	0.26, <i>0.33 (+28%)</i>	0.94, <i>0.17</i>	0.18, <i>0.28 ($\times 1.6$)</i>

The decrease in ^{134}Ba results in an overall decrease of the $^{134}\text{Ba}/^{136}\text{Ba}$ isotopic ratio, with the geometric average of all the models shown in Table 1 changing from 16% higher than solar using the old rate, to 16% lower than solar using the new rate. However, a proper comparison with the solar abundances can only be accomplished by running full galactic chemical evolution models.

For the final s -process ^{135}Ba abundance, the geometric average of all the models shown in Table 1 is higher by 30% when using the new rate, relatively to using the TY87 rate, although a full galactic chemical evolution calculation is needed to derive the accurate number. Such variation results in a small decrease of roughly 12% in the r -process residual abundance of ^{135}Ba . When added to the present error bars of roughly 9%, based on uncertainties on the neutron-capture cross section and the solar abundance ([Arlandini et al. 1999](#)), the value of the r -process residual abundance of ^{135}Ba may be up to 20% lower than used usually. Considering, for example, Figure 6 of [Vockenhuber et al. \(2007\)](#), this decrease would move the r -process residual abundance of ^{135}Ba to just below that of ^{137}Ba , while one would expect ^{135}Ba to be above ^{137}Ba . A full analysis of the branching points along the Cs isotopes leading also to the production of ^{137}Ba is needed to evaluate and resolve this possible tension. If the second r -process peak (at $A \sim 130$) results in being reshaped and potentially narrowed by the lower ^{135}Ba residual derived using our new rate, this will have implications on our understating of the fission recycling during the r process ([Kajino et al. 2019](#); [Mumpower et al. 2018](#)).

In Figure 4 we present the comparison between our model predictions and the composition of single stardust SiC grains measured with Resonant Ionisation Mass Spectrometry (RIMS, see [Liu et al. 2014](#), and references therein). We focus in this figure on the models with solar and higher-than-solar metallicity, as these has been reported previously to provide the best match to the SiC data ([Lugaro et al. 2018a](#); [Liu et al. 2018](#), e.g.). They are the same models used by

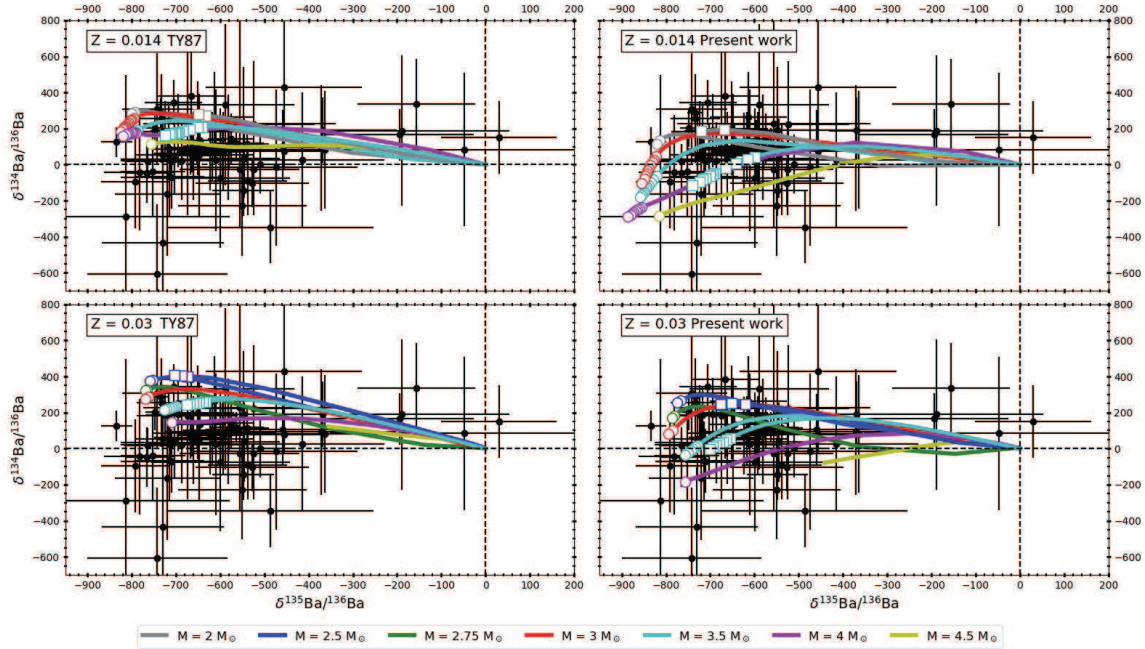


Figure 4. Comparison between data for single stardust SiC grains (black dots with 2σ error bars, from Liu et al. 2014) and AGB model predictions of different masses, metallicities, and decay rates of ^{134}Cs , as indicated by the labels, where $Z = 0.014$ is the solar metallicity, TY87 is the rate from Takahashi & Yokoi (1987) and “Present work” refers to the new rate presented in this paper. The data are plotted using the standard δ notation, where $\delta^{134,135}\text{Ba}/^{136}\text{Ba}$ represents the permil variation of the ratio with respect to solar. The model predictions start at solar composition ($\delta = 0$) and follow the coloured lines until the envelope becomes C-rich (the condition for the formation of SiC) and open symbols are plotted. This means that the SiC data points should be compared exclusively to the open symbols. Circles represent models where the extent in mass M_{PMZ} of the mixing of protons leading to the formation of the ^{13}C neutron source was taken to be the standard reported in Table 1 of Lugaro et al. (2018a). Squares represents models where M_{PMZ} was reduced by a factor of 10 in the $Z=0.014$ models and by a factor of 2 in the $Z=0.03$ models.

Lugaro et al. (2018a) and more details on their structural features can be found in Table 1 of that paper. As discussed above, the models calculated with the new ^{134}Cs decay rate result in lower $^{134}\text{Ba}/^{136}\text{Ba}$ ratios, which, when compared to the grain data, provide a general better fit to the observed spread. The new models reach down to cover, within the error bars, the two grains most strongly depleted in ^{134}Ba which were previously unexplained and potentially attributed to the operation of the intermediate neutron capture (i process) in post-AGB stars (Liu et al. 2014), suggesting that the two grains could still be explained by the s process alone. Due to its being already significantly lower than solar, the predicted lines for the $^{135}\text{Ba}/^{136}\text{Ba}$ ratio are only marginally shifted to the left due to the new rate. The grain data indicates a spread of $^{135}\text{Ba}/^{136}\text{Ba}$ ratio with values towards the solar value. This spread can be predicted when changing the free parameter in the models which represents the extent in mass of the region of partial mixing (M_{PMZ}) leading to the formation of the ^{13}C neutron source (Karakas & Lugaro 2016; Lugaro et al. 2018a). In the case of the solar metallicity models we needed to divide M_{PMZ} by a factor of 10, in the case of the models of twice-solar metallicity it was enough to reduce this mass by a factor of two to derive a better match to the measured $^{135}\text{Ba}/^{136}\text{Ba}$ ratios. The difference is due to the models of lower metallicity being more efficient in producing the s -process isotopes, such as ^{136}Ba , because of the lower number of Fe seeds (Clayton 1988). Finally we note that for this comparison we considered the ^{135}Ba abundance alone, without the contribution of ^{135}Cs . This assumes that SiC condenses in AGB envelopes within a few Myr, i.e., before a significant amount of ^{135}Cs has decayed into ^{135}Ba , and that Cs does not condense into SiC, since it is a relatively volatile element. Our models support this assumptions, which was already discussed in Lugaro et al. (2003) (see their Figure 16), and even more strongly when considering the predictions obtained using the new decay rate of ^{134}Cs .

While our new rate has direct and indirect implications on the s - and r -process, respectively, it is not expected to lead to significant modification of the Ba isotopic abundances produced by the i process, with neutron densities of the order of $10^{13} - 10^{15} \text{ cm}^{-3}$, in-between those of the s and r processes. This is because during the i process the Ba isotope most produced is ^{135}Ba , resulting from the decay of the neutron magic unstable ^{135}I (see, e.g., Figure 1 of Hampel et al. (2016)). The behavior of the Cs branching points represents a less significant effect relative to this major feature of the i process.

There are also potential implications of our results for the early Solar System. Long-lived radioactive isotopes have been found to be present at the time of the formation of the first solids at the birth of the Sun, however, for $^{135}\text{Cs}/^{133}\text{Cs}$ ratio only an upper limit of 2.8×10^{-6} (Brennecka & Kleine 2017) is available. This means that from this upper limit we can only derive a lower limit for the time elapsed from the last AGB nucleosynthetic event that polluted the pre-solar system matter to the birth of the Sun (Lugaro et al. 2014). For consistency with (Lugaro et al. 2014, 2018b) we consider the $3 M_{\odot}$, $Z=0.014$ model as typical, and calculated the time that elapsed from the last AGB events using Eq. 15 of Lugaro et al. (2018b) with the Galactic chemical evolution parameter $K=2.3$ (Côté et al. 2019a) and with the time interval between polluting events of 50 Myr to ensure that we are in the regime where it is only one event that contributed to the early Solar System abundances of the long-lived isotopes produced by AGB stars (Côté et al. 2019b). We derive elapsed times of the order of 32-38 Myr from ^{107}Pd and ^{182}Hf . For ^{135}Cs we derive an elapsed time >24 Myr and >28 Myr when considering the $^{135}\text{Cs}/^{133}\text{Cs}$ ratios predicted using the ^{134}Cs decay rate by TY87 and the present work, respectively. In both cases agreement is found with the other two long-lived isotopes.

Finally, we examined the impact of the new decay rate on the ratio f_{odd} between the abundances of the odd-A and even-A isotopes of Ba. In most of our models f_{odd} is very close to traditional s -process reported value of $f_{\text{odd}} = 0.11$ (Arlandini et al. 1999). The changes are at most a increase of 15% when considering the new decay rate.

4. SUMMARY

The stellar β -decay rate of the branching point ^{134}Cs is crucial to the understanding of s -process nucleosynthesis at the vicinity of $^{134-136}\text{Ba}$. Large-scale shell-model calculations were performed to determine the GT strengths of the important transitions from the ^{134}Cs excited states to the excited and ground states of ^{134}Ba . At typical s -process temperatures, the new decay rate from our calculation is significantly lower than the TY87 rate estimated with empirical $\log ft$ values. With the new β -decay rate, we performed nucleosynthesis calculations using AGB stellar models with various masses and metallicities. Our result shows an overall decrease in the s -only $^{134}\text{Ba}/^{136}\text{Ba}$ isotopic ratio and well explains the $^{134}\text{Ba}/^{136}\text{Ba}$ isotopic ratios in meteorites without introducing the i process at the post-AGB phase. We also derive the elapsed time from the last AGB nucleosynthetic event that polluted the early Solar System to be >28 Myr based on the $^{135}\text{Cs}/^{133}\text{Cs}$ ratio, consistent with the elapsed times derived from ^{107}Pd and ^{182}Hf . The abundance sum of ^{135}Ba and ^{135}Cs is found to increase, resulting in a smaller r -process contribution of ^{135}Ba to the Solar System. The remaining uncertainty of the ^{134}Cs stellar decay rate mainly comes from the tentative spin-parity assignment of some low-lying states. The spin-parity assignments are essential to match shell model levels with experimental levels, and incorrect assignments would yield incorrect matching. Experimental investigation of the spin-parity structure of ^{134}Cs is therefore key to a precise understanding of multiple astrophysical nucleosynthesis sites in this mass region.

This project is supported by the Strategic Priority Research Program of Chinese Academy of Sciences, Grant No. XDB34020000, the national key research and development program (MOST 2016YFA0400501), the ERC Consolidator Grant (Hungary) funding scheme (Project RADIOSTAR, G.A. n. 724560), the ISSI-Beijing project "Radioactive Nuclei in the Cosmos and in the Solar System" and the Chinese and Hungarian Academy of Sciences visitor exchange program. C.Q. was supported by the Swedish Research Council (VR) under grant Nos. 621-2012-3805, and 621-2013-4323 and the Göran Gustafsson foundation. The calculations were performed on resources provided by the Swedish National Infrastructure for Computing (SNIC) at PDC at KTH, Stockholm. A.I.K. was supported by the Australian Research Council Centre of Excellence for All Sky Astrophysics in 3 Dimensions (ASTRO 3D), through project number CE170100013. X.T. acknowledges support from the National Natural Science Foundation of China under Grant No. 11021504, 11321064, 11475228 and 11490564, 100 talents Program of the Chinese Academy of Sciences. X.T. thanks Hayden Campbell for proofreading.

REFERENCES

- Arlandini, C., Käppeler, F., Wisshak, K., et al. 1999, *ApJ*, 525, 886
- Asplund, M., Grevesse, N., Sauval, A. J., & Scott, P. 2009, *ARA&A*, 47, 481
- Bisterzo, S., Gallino, R., Käppeler, F., et al. 2015, *MNRAS*, 449, 506
- Bogdanović, M., Brissot, R., Barreau, G., et al. 1987, *NuPhA*, 470, 13
- Bojazi, M. J., & Meyer, B. S. 2014, *PhRvC*, 89, 025807
- Brennecke, G. A., & Kleine, T. 2017, *ApJL*, 837, L9
- Cannon, R. C. 1993, *MNRAS*, 263, 817
- Clayton, D. D. 1988, *MNRAS*, 234, 1
- Côté, B., Lugaro, M., Reifarth, R., et al. 2019a, *ApJ*, 878, 156
- Côté, B., Yagüe, A., Világos, B., & Lugaro, M. 2019b, *ApJ*, 887, 213
- Cristallo, S., Straniero, O., Gallino, R., et al. 2009, *ApJ*, 696, 797
- Cristallo, S., Piersanti, L., Straniero, O., et al. 2011, *ApJS*, 197, 17
- Fishlock, C. K., Karakas, A. I., Lugaro, M., & Yong, D. 2014, *ApJ*, 797, 44
- Gallino, R., Arlandini, C., Busso, M., et al. 1998, *ApJ*, 497, 388
- Goriely, S. 1999, *A&A*, 342, 881
- Hempel, M., Stancliffe, R. J., Lugaro, M., & Meyer, B. S. 2016, *ApJ*, 831, 171
- Hjorth-Jensen, M., Kuo, T. T. S., & Osnes, E. 1995, *PhR*, 261, 125
- KADoNis. v0.3, Karlsruhe Astrophysical Database of Nucleosynthesis in Stars. <http://www.kadonis.org/>
- Kajino, T., Aoki, W., Balantekin, A. B., et al. 2019, *Progress in Particle and Nuclear Physics*, 107, 109
- Karakas, A. I. 2014, *MNRAS*, 445, 347
- Karakas, A. I., & Lattanzio, J. C. 2014, *PASA*, 31, e030
- Karakas, A. I., & Lugaro, M. 2016, *ApJ*, 825, 26
- Karakas, A. I., Lugaro, M., Carlos, M., et al. 2018, *MNRAS*, 477, 421
- Liu, N., Gallino, R., Cristallo, S., et al. 2018, *ApJ*, 865, 112
- Liu, N., Savina, M. R., Davis, A. M., et al. 2014, *ApJ*, 786, 66
- Lugaro, M., Davis, A. M., Gallino, R., et al. 2003, *ApJ*, 593, 486
- Lugaro, M., Karakas, A. I., Petó, M., & Plachy, E. 2018a, *GeoCoA*, 221, 6
- Lugaro, M., Karakas, A. I., Stancliffe, R. J., & Rijs, C. 2012, *ApJ*, 747, 2
- Lugaro, M., Ott, U., & Kereszturi, Á. 2018b, *Progress in Particle and Nuclear Physics*, 102, 1
- Lugaro, M., Heger, A., Osrin, D., et al. 2014, *Science*, 345, 650
- Machleidt, R. 2001, *PhRvC*, 63, 024001
- Mumpower, M. R., Kawano, T., Sprouse, T. M., et al. 2018, *ApJ*, 869, 14
- NNDC. 2021, National Nuclear Data Center. <http://www.nndc.bnl.gov>
- Patronis, N., Dababneh, S., Assimakopoulos, P. A., et al. 2004, *PhRvC*, 69, 025803
- Qi, C., & Xu, Z. X. 2012, *PhRvC*, 86, 044323
- Takahashi, K., & Yokoi, K. 1987, *Atomic Data and Nuclear Data Tables*, 36, 375
- Travaglio, C., Galli, D., Gallino, R., et al. 1999, *ApJ*, 521, 691
- Vockenhuber, C., Dillmann, I., Heil, M., et al. 2007, *PhRvC*, 75, 015804